Research on Concrete Columns Reinforced with New Developed High-Strength Steel under Eccentric Loading

Yonghui Hou[1,2], Shuangyin Cao[1,2,*], Xiangyong Ni[1,2], Yizhu Li[1,2]

[1] Key Laboratory of Concrete and Prestressed Concrete Structures of Ministry of Education, Southeast University, Nanjing, P.R. China

[2] School of Civil Engineering, Southeast University, Nanjing, P.R. China

* Corresponding author (Shuangyin Cao), Professor, E-mail: 101000873@seu.edu.cn

Abstract: The use of new developed high-strength steel in concrete members can reduce steel bars congestion and construction costs. This research aims to study the behavior of concrete columns reinforced with new developed high-strength steel under eccentric loading. Ten reinforced concrete columns were fabricated and tested. The test variables are transverse reinforcement amount and yield strength, eccentricity, and longitudinal reinforcement yield strength. The failure patterns are compression and tensile failure for columns subjected to small eccentricity and large eccentricity, respectively. The same level of post-peak deformability and ductility only can be obtained with lower amount of transverse reinforcement when high-strength transverse reinforcements are used in columns subjected to small eccentricity. The high-strength longitudinal reinforcement can improve bearing capacity and post-peak deformability of concrete columns. Besides, three different equivalent rectangular stress block (ERSB) parameters in predicting bearing capacity of columns with high-strength steel were discussed based on test and simulated results. It is concluded that the Code of GB 50010-2010 overestimates the bearing capacity of columns with high-strength steel, whereas bearing capacities computed using Codes of ACI 318-14 and CSA A23.3-04 agree well with test results.

Keywords: concrete columns; eccentric loading; high-strength steel; ductility; bearing capacity

1 Introduction

In last decade, using high-strength steel bars in construction industry has promoted the extensive research in this area. The high-strength steel bars have the merit to lower reinforcement congestion and construction costs, especially in high-rise and special buildings. The use of high-strength steel as longitudinal reinforcement can enhance concrete members' load capacity, moreover, its use for stirrups may decrease transverse reinforcement amount required to ease concrete placement. In recently years, the continuous development of steel smelting technology has produced new high-strength steel (for example, Grade 100 in USA, Grade 600 in Korea and HRB600 in China). The new developed high-strength steel has a linear pre-yield behavior, obvious yield plateau and comparatively good ductility, while the ultra-high-strength reinforcing bar has high yield strength, but no yield plateau and poor ductility. The typical stress-strain relationships of different reinforcing bars are presented in Fig.1. The yield plateau of new developed high-strength steel is much shorter than that of conventional steel, and the rupture elongation of new developed high-strength steel is approximately 70% of that of conventional steel. Therefore, the new developed high-strength steel with changed mechanical properties has an obvious effect on the performance of concrete members.

There have been many investigations on the performance of high-strength steel (including high-strength longitudinal reinforcement and transverse reinforcement) used in concrete beams [1-3], beam-column joints [4-6], and walls [7-8]. As a result, using high-strength steel has become widespread in concrete structural application. However, limited researches have been carried out to obtain eccentric compressive behavior of concrete columns

Peer-reviewed version available at Materials 2019, 12, 2139; doi:10.3390/ma12132139

reinforced with high-strength steel, although many scholars [9-14] have conducted studies on high-strength steel used in concrete columns.

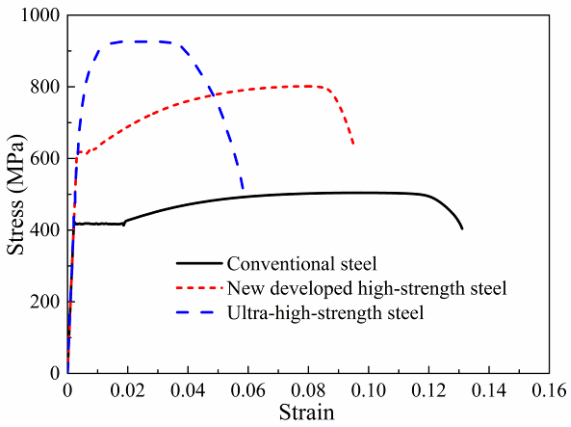

Fig.1. Stress-strain relationships of different reinforcing bars

Many researchers [15-17] have carried out the axial compression tests on concrete columns confined by high-strength transverse reinforcements and demonstrated that using high-strength stirrups can improve ductility behavior of column and result in reduced steel congestion during construction. Paultre et al. [18] and Xiao et al. [19] performed experimental study on concrete columns confined with high-strength transverse reinforcements under reversed cyclic loading and mentioned that seismic behavior of columns increased. Moreover, high-strength transverse reinforcement could effectively confine concrete while reducing transverse reinforcement amount. Rautenberg et al. [9-10] studied eight concrete columns reinforced with high-strength longitudinal reinforcements under displacement reversals and determined that columns reinforced with high-strength longitudinal reinforcements presented similar flexural bearing capacity, deformability, but lower energy-dissipating capacity as compared with columns reinforced by conventional steel. The similar results on seismic behavior of slender columns reinforced with high-strength longitudinal reinforcements also can be found in the research literatures [14, 20-21]. Ou et al. [11-12] and Sokoli et al. [13] studies the shear behavior of large-scale concrete columns reinforced by high-strength steel and concluded that bond degradation around the longitudinal reinforcement occurred and the shear strength of columns was affected by axial compression. This suggests that the minimum shear reinforcement equation need to consider the influence of axial compression.

The previous available literatures on the use of new developed high-strength steel mainly focus on seismic behavior of concrete beams, columns, beam-column joints and walls, while the study on the eccentric compressive behavior of columns reinforced with new developed high-strength steel is insufficient. This research investigated the behavior of new developed high-strength steel used in concrete columns under eccentric loading. Ten large-scale concrete square columns with high-strength steel were design to explore the effect of using new developed high-strength steel. In additions, this paper also compares the different analytical models to predict the axial load-bending moment interaction curves of high-strength steel reinforced square concrete columns.

2 Experimental Program

2.1 Test specimens

Ten concrete columns were designed and fabricated with a square section (350×350 mm) and the height of column was 1500 mm. The test region of columns with height of 700 mm and two column ends (each 400 mm in height) were haunched. The concrete cover thickness of columns was 20 mm. Test regions of columns were constructed using 12-D16 longitudinal reinforcements, and the percentage of longitudinal reinforcements (ρ_l) was 1.97%. The columns were confined by well-shaped compound hoops with 135-degree bend anchorages. Transverse reinforcement spacing in test region was 70 mm or 105 mm, and the corresponding transverse

reinforcement ratio (ρ_{sh}) were 1.91% and 1.28%, respectively. The two haunched heads were fabricated with dense transverse reinforcements of 50 mm to prevent local compression failure at column ends. The geometric sizes and reinforcing bars of columns are illustrated in Fig.2, and Table 1 presents the test parameters in detail.

Table 1 Test design parameters

Column	Concrete	Eccentricity	Longitudinal reinforcement			Transverse reinforcement					
	f_c'(MPa)	e (mm)	No.-size	f_{yl}(MPa)	ρ_l (%)	Size	Spacing(mm)	f_{yh}(MPa)	ρ_{sh}(%)	$\rho_{sh}f_{yh}/f_c$'	$\rho_{sh}/\rho_{sh(ACI)}$
EC1	36.5	75	12-D16	446	1.97	D8	70	476	1.91	0.296	1.27
EC2	36.5	74	12-D16	446	1.97	D8	70	642	1.91	0.399	1.72
EC3	36.5	80	12-D16	446	1.97	D8	105	642	1.28	0.268	1.15
EC4	36.5	79	12-D16	617	1.97	D8	70	642	1.91	0.399	1.72
EC5	36.5	75	12-D16	617	1.97	D8	105	642	1.28	0.268	1.15
EC6	36.5	177	12-D16	446	1.97	D8	70	476	1.91	0.296	1.27
EC7	36.5	180	12-D16	446	1.97	D8	70	642	1.91	0.399	1.72
EC8	36.5	176	12-D16	446	1.97	D8	105	642	1.28	0.268	1.15
EC9	36.5	179	12-D16	617	1.97	D8	70	642	1.91	0.399	1.72
EC10	36.5	179	12-D16	617	1.97	D8	105	642	1.28	0.268	1.15

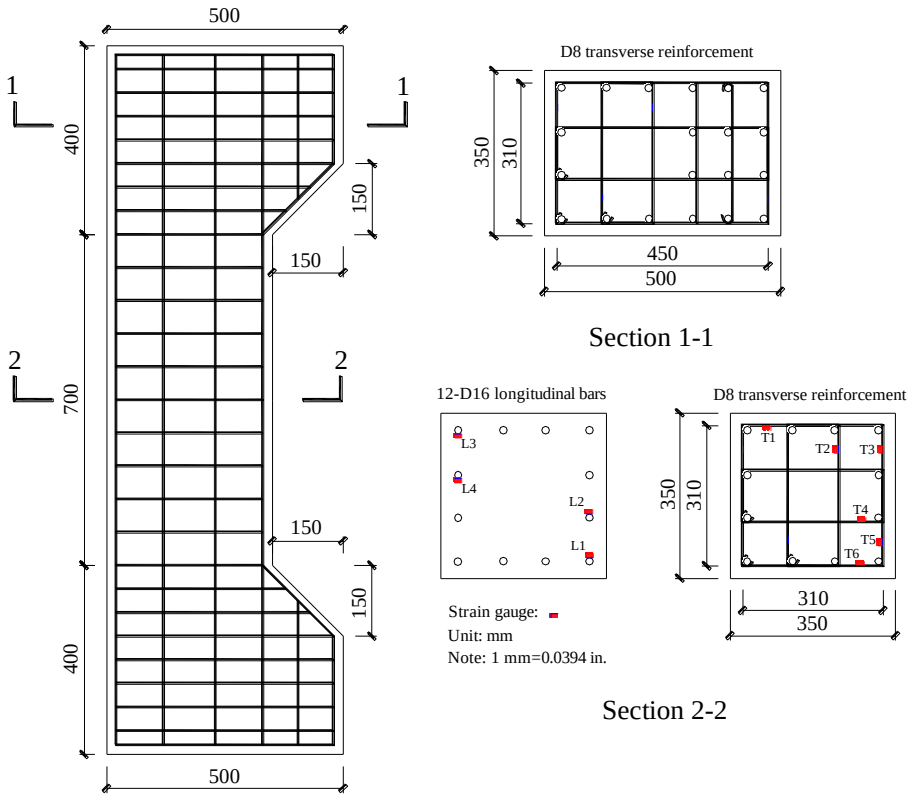

Fig.2 Geometric sizes and reinforcement details

2.2 Test variables

This test aims to study three main variables that affect the eccentric compressive behavior of concrete columns: 1) effect of using high-strength transverse reinforcement; 2) effect of using high-strength longitudinal reinforcements; 3) effect of eccentricity. Clause 18.7.5.3 in ACI 318-14 [22] specified the limits for transverse reinforcement spacing. The transverse reinforcement spacing should not exceed: 1) a quarter of minimum member cross-sectional dimension, 2) six times the longitudinal bar diameter, and 3) s_o as defined by Eq. (18.7.5.3). These limitations lead to maximum transverse reinforcement spacing of 87.5 mm for columns. Four specimens, EC3, EC5, EC8 and EC10, do not meet the ACI 318-14 requirement on maximum transverse reinforcement spacing. All

columns were separated into two parts. The first part consisted of five concrete columns (EC1, EC2, EC3, EC4, and EC5). Columns of the first part were loaded under a nominal eccentricity of 80 mm (e/h=0.23). In the second part a total of five concrete columns (EC6, EC7, EC8, EC9, and EC10) were examined under a nominal eccentricity of 180 mm (e/h=0.51). The detailed test variables are presented in Table 1.

Columns EC2 and EC6 reinforced with D8 high-strength transverse reinforcement and had same transverse reinforcement configuration with Columns EC1 and EC5 reinforced by ordinary transverse reinforcement to investigate effects of transverse reinforcement yield strength. The ratio of configured high-strength stirrup amount to the amount specified by ACI 318-14 [22] was 1.72. Whereas the ratio of configured ordinary stirrup amount to the amount required by ACI 318-14 was 1.27. Columns EC3 and EC7 confined by high-strength stirrup but with reduced amount compared with previous four columns were designed to understand the effects of high-strength transverse reinforcement amount.

Columns EC4, EC5, EC9 and EC10 were confined by same transverse reinforcement configuration as Columns EC2, EC3, EC7 and EC8, respectively, but only differed in longitudinal reinforcement yield strength. Columns EC4, EC5, EC9 and EC10 were fabricated with high-strength longitudinal reinforcements as comparison Columns EC2, EC3, EC7 and EC8 reinforced with ordinary longitudinal reinforcements. Comparison of the behavior of these columns is aim to understand the influences of high-strength longitudinal reinforcement.

2.3 Material properties

All columns were casted using same batch concrete mixes. The materials involved Portland cement, river sand, coarse aggregate, tap water of mixing and curing, fly ash and mineral powder to improve workability of material. The ratio of sand to aggregate was 0.36 and the water-bind ratio was 0.32. Little superplasticizer was mixed to increase concrete fluidity. Six plain concrete cubes with wide 150 mm were fabricated and tested on the day of columns loading to obtain average concrete compressive strength f_c' according to the Code of GB50010-2010, as shown in Table 1.

D16 HRB400 and D16 HRB600 reinforcing bars were served as longitudinal reinforcements. The HRB400 and new developed HRB600 represent minimum specified yield strength of 400 MPa and 600 MPa, respectively. All columns were confined by D8 HRB400 or HRB600 transverse reinforcement. Tensile tests of steel samples were conducted to obtain properties of each type of reinforcing bars. The detailed of reinforcing bars are given in Table 2.

Table 2 Properties of reinforcing bars

	Size	Grade	Elasticity modulus (MPa)	Yield strength (MPa)	Yield strain	Ultimate strength (MPa)
Longitudinal reinforcement	D16	HRB400	2.08×10^5	446	0.0021	585
	D16	HRB600	2.05×10^5	617	0.0030	802
Transverse reinforcement	D8	HRB400	2.00×10^5	476	0.0024	635
	D8	HRB600	2.04×10^5	642	0.0031	803

2.4 Test setup and loading

All columns were subjected to eccentric loading using a 10,000 kN capacity electro-hydraulic servo machine, as shown in Fig.3. The top ends of columns were connected with electro-hydraulic actuator and the lower ends were placed on the steel block. Both ends of columns were designed as hinge connection. The columns were loaded with 0.02 mm/s until the end of test. Five linear voltage differential transducers (LVDTs) were installed along the height of column to measure lateral deformation. Two of LVDTs were fixed near the column ends, and a LVDT installed at the mid-height of column to obtain the maximum flexural deflection. The remaining two LVDTs were placed at the approximate one quarter and three quarters of column height, respectively. The detailed instrumentations are illustrated in Fig.3. Strain foil was used to measure the strains in reinforcing bars. The strain foil of longitudinal reinforcements and transverse reinforcements were installed at test region, and the detailed locations are illustrated in Fig.2.

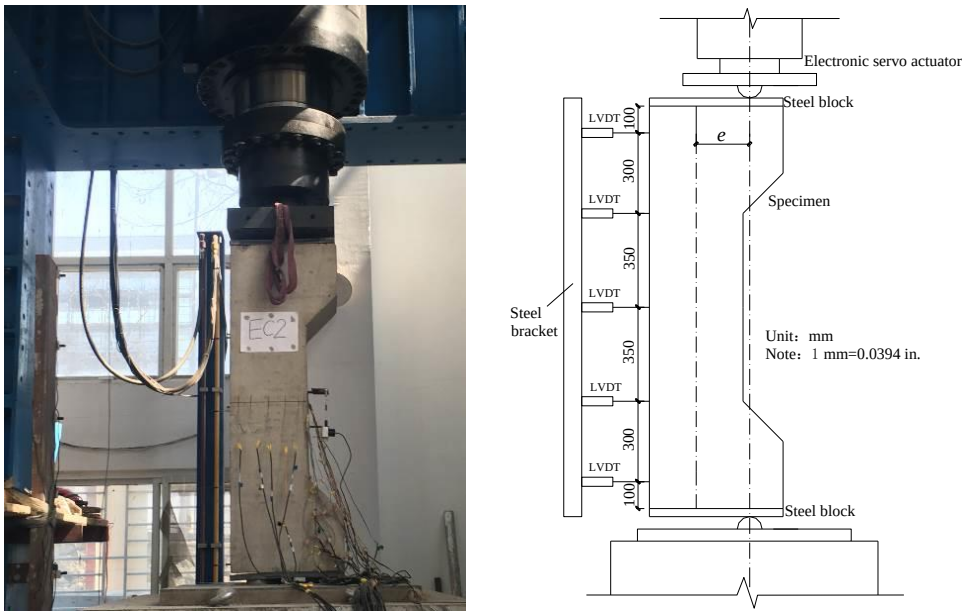

Fig.3 Typical test setup and instrumentation

3 Experimental Results

3.1 Failure patterns

The columns subjected to small-eccentric compressive loading (nominal *e*=80 mm) failed at the mid-height, as demonstrated in Fig. 4(a). The failure patterns of five columns are similar, appearing compression failure despite of high-strength steel used in columns. At the beginning of loading, most of cross-section regions of columns are compressive. As the displacement increases, the concrete at compression-side crushed suddenly, and followed by buckling outward of longitudinal reinforcement (Fig. 4(b)). The failure of columns is determined by concrete compression crushing at compression-side. Under the small eccentric compression loading, tensile cracks were observed but did not extend to the entire cross-section of column (Fig. 4(c)). This is because the confinement effect caused by transverse reinforcement limits the development of cracks, which generates the core concrete be triaxial compression status. Thus, the failure pattern of columns with small eccentricity is concrete crushing at compression-side.

The columns subjected to large-eccentric compressive loading (nominal *e*=180 mm) also failed at the mid-height of columns, as given in Fig. 4(d). The breakings of five columns are almost similar and present typical tensile failure pattern, which caused by large bending moment at mid-height of column. The bending moment at mid-height promoted the start of concrete cracking. As the load increases, the tensile cracks propagated from the outside of cross-section to the inside. Finally, the tensile cracks extend to the entire cross-section of columns with several major cracks at the tensile zones (Fig. 4(e)) and concrete crushed at the compression-side. The longitudinal reinforcements at the compression-side buckled and concrete in the middle of cross-section cracked and peeled off slowly, which can be observed in Fig. 4(f). For columns with different reinforcing bars amount and yield strength, the failure patterns and post-peak deformability of columns did not change significantly.

(a) Final failure mode

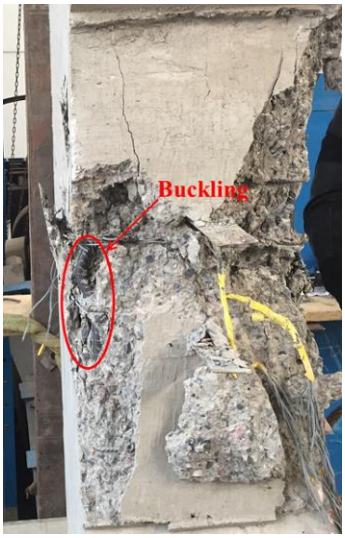

(b) buckling of longitudinal bar

(c) Tensile cracks

(d) Final failure mode of EC6

(e) Major cracks

(f) Final failure mode of EC8

Fig.4 Failure patterns of columns

3.2 Load-displacement behavior

The lateral displacement verses applied load curves for columns are illustrated in Fig.5. The lateral displacement was obtained from LVDT placed at the mid-height. All columns have an approximate linear load-displacement curve up to yield point, that the longitudinal reinforcement yielded, and the lateral displacement is approximately 4 mm for columns loaded to small eccentricity (e=80 mm), and it is 5.5 mm for columns subjected to large eccentricity (e=180 mm). After yield point, the plastic hinge is generated near the mid-height and the stiffness of columns decreased. This behavior is continued until the concrete cover crushing and spalling, which caused a sudden decrease of approximately 5% to 10% of maximum load. The average lateral displacement is 9.0 mm when first peak load reach. The applied load increased again until a second peak appeared for strongly-confined columns only (e.g. EC1, EC2 and EC9), and the corresponding lateral displacement ranged from 13.1 mm to 13.95 mm. For columns loaded to small eccentricity (e=80 mm), the post-peak deformability was less than that of columns subjected to large eccentricity (e=180 mm), and post-peak behavior was similar with the response of columns under the concentric compression loading. The transverse reinforcements provide lateral confinement effect to core concrete, and increase the deformability of columns. Therefore, the transverse reinforcement amounts and yield strength have significant effects on the confinement effect of concrete and dominated post-peak behavior of columns. For columns loaded to large eccentricity (e=180 mm), the post-peak behavior was similar with response of flexural member, and they failed in ductility behavior. The compression

zones of the critical cross-section for columns were relatively small and transverse reinforcements did not develop lateral confining pressure. Therefore, the effects of transverse reinforcement amounts and yield strength on behavior of columns were slightly.

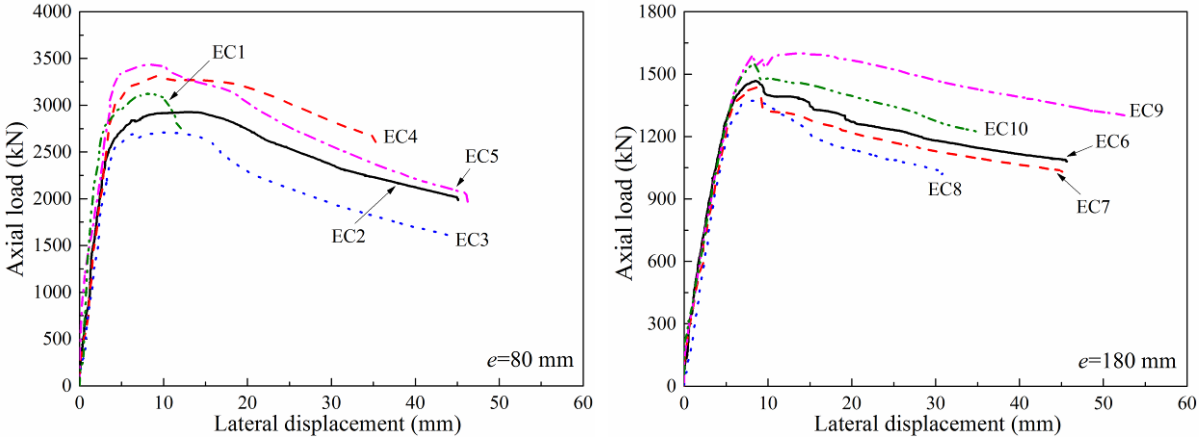

(a) Nominal eccentricity e=80 mm (b) Nominal eccentricity e=180 mm

Fig.5 Load-displacement curves of columns

3.3 Lateral deformation

The lateral deformations recorded by five LVDTs are illustrated in Fig.6. The lateral deformation of columns presented similar shape at different applied loading. Especially, the lateral displacements of columns increased significantly when the applied load increased to maximum load. The lateral displacements of columns subjected to large eccentricity were larger than those of columns subjected to small eccentricity at different loading stage. The lateral deformation of columns is caused by bending moment and often assumed to a sine-shaped [23-24], the expression is as follows:

$$\delta = \Delta \sin(\frac{\pi x}{L}) \qquad (1)$$

where Δ is the lateral displacement at mid-height of column; x is the longitudinal coordinate variable, as shown in Fig.6; L is the height of column; and δ is the lateral displacement at the x position, as given in Fig.6.

Comparison of the sin-shaped model with experimental lateral deformation is shown in Fig.6. It indicates that the sine-shaped model agrees well with experimental data for column cross section of 350 mm×350 mm. This model provides a good prediction for the lateral deformation of columns at different level of deformation. Thus the sine-shaped model can be applied to RC columns with high-strength steel.

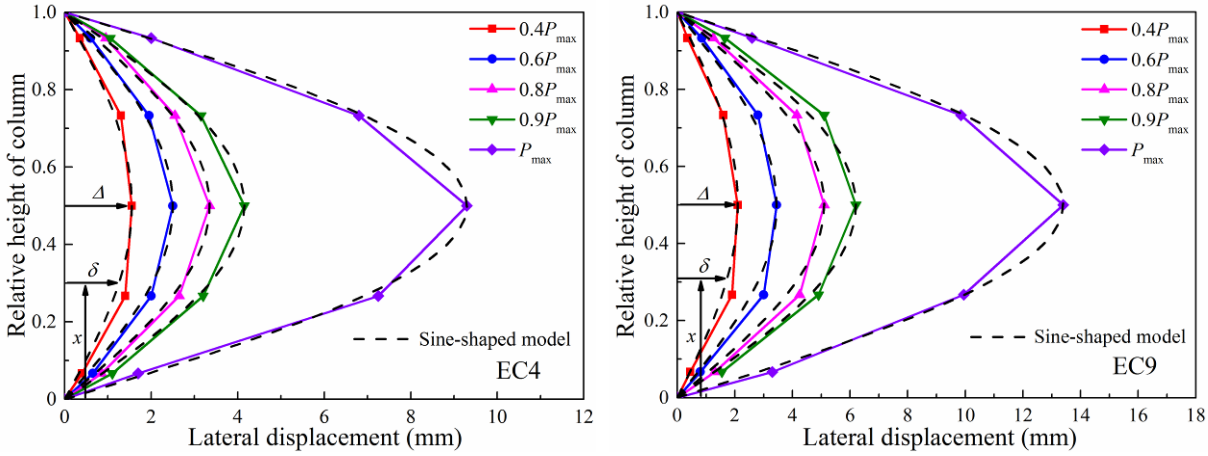

(a) (b)

Fig.6 Lateral deformation of columns: (a) EC4 (e=79 mm); (b) EC9 (e=179 mm)

3.4 Measured strains in longitudinal and transverse reinforcement

Table 3 summarizes the load at first yielding of longitudinal reinforcement and steel strains at the maximum

load (P_{max}). The first longitudinal reinforcement yielding appeared at the compression-side of columns subjected to small eccentricity (e=80 mm), while it happened at the tension-side of columns subjected to large eccentricity (e=180 mm). The steel yielding appeared at 0.779P_{max} on average, ranging from 0.712 to 0.831P_{max}, for columns reinforced with ordinary longitudinal reinforcements and at 0.904P_{max} on average, ranging from 0.845 to 0.938P_{max}, for columns with high-strength longitudinal reinforcements. At maximum load, the average ratios ($\varepsilon_{lc,Pmax}/\varepsilon_y$) of measured strain to yield strain in compressive longitudinal reinforcements for columns ranged from 4.00 to 10.95, which indicate that the compressive longitudinal reinforcements could yield despite of the use of high-strength longitudinal reinforcement. Whereas the average ratios ($\varepsilon_{lt,Pmax}/\varepsilon_y$) of measured strain to yield strain in the tensile longitudinal reinforcements ranged from 0.67 to 1.86 for columns subjected to small eccentricity and ranged from 1.50 to 5.24 for columns subjected to large eccentricity, which indicate that the tensile high-strength longitudinal reinforcements could not yield ($\varepsilon_{lt,Pmax}/\varepsilon_y$=0.67/0.90) for columns loaded to small eccentricity. The average strains ($\varepsilon_{hc,Pmax}$) of transverse reinforcement in compression-side ranged from 1.03 to 2.03 of yield strain of transverse reinforcement for columns subjected to small eccentricity, which is similar to the behavior of columns subjected to concentric compression loading. It indicates that transverse reinforcements have obvious confinement effect on concrete. While the average strain ($\varepsilon_{hc,Pmax}$) of transverse reinforcement in compression-side ranged from 0.39 to 0.79 of yield strain for columns loaded to large eccentricity, which show that confinement effect of transverse reinforcement on core concrete was not significant due to the low stress of transverse reinforcements. The average strains ($\varepsilon_{ht,Pmax}$) of transverse reinforcement in tension-side ranged from 0.02 to 0.39 of yield strain of transverse reinforcement for all columns, which is much less than the yield strain. This is due to the stress release of transverse reinforcement caused by cracking of concrete in tension-side.

Table 3 Measured strains in longitudinal and transverse reinforcement

Column	P_{max} (kN)	Load at first yielding of longitudinal bar		Average strains in longitudinal bar				Average strains in transverse reinforcement			
		P_{yl} (kN)	P_{yl}/P_{max}	$\varepsilon_{lt,Pmax}$	$\varepsilon_{lt,Pmax}/\varepsilon_y$	$\varepsilon_{lc,Pmax}$	$\varepsilon_{lc,Pmax}/\varepsilon_y$	$\varepsilon_{ht,Pmax}$	$\varepsilon_{ht,Pmax}/\varepsilon_y$	$\varepsilon_{hc,Pmax}$	$\varepsilon_{hc,Pmax}/\varepsilon_y$
EC1	3125	2423	0.775	0.0030	1.43	0.014	6.67	0.0002	0.083	0.0031	1.29
EC2	2927	2380	0.813	0.0039	1.86	0.014	6.67	0.0012	0.387	0.0063	2.03
EC3	2709	2250	0.831	0.0028	1.33	0.015	7.14	0.0003	0.097	0.0036	1.16
EC4	3311	2798	0.845	0.0020	0.67	0.015	5.00	0.0009	0.290	0.0032	1.03
EC5	3434	3223	0.938	0.0027	0.90	0.014	4.67	0.0004	0.129	0.0034	1.10
EC6	1467	1166	0.790	0.0110	5.24	0.020	9.52	0.0004	0.167	0.0019	0.79
EC7	1437	1023	0.712	0.0087	4.14	0.019	9.05	0.0003	0.097	0.0014	0.45
EC8	1373	1031	0.751	0.0085	4.05	0.023	10.95	0.0003	0.097	0.0015	0.48
EC9	1599	1452	0.908	0.0045	1.50	0.017	5.67	0.0006	0.019	0.0022	0.71
EC10	1549	1429	0.923	0.0045	1.50	0.012	4.00	0.0004	0.129	0.0012	0.39

3.5 Summary of test results

Table 4 summarizes the test results, including the maximum load P_{max} and corresponding mid-height lateral displacement Δ_{max}, calculated maximum loads P_{ACI}, P_{GB} and P_{CSA} using Codes of ACI 318-14 [22], GB 50010-2010 [25] and CSA A23.3-04 [26] respectively, yield displacement Δ_y and the displacements $\Delta_{0.85P}$ corresponding to 0.85 of maximum load. The maximum loads of columns were calculated using the equivalent rectangular stress block (ERSB) parameters stated in ACI 318-14, GB 50010-2010 and CSA A23.3-04. ACI 318-14 defines ERSB width and depth using parameters α and β, respectively. Factor α shall be given as 0.85. The concrete ultimate compression strain is taken as ε_{cu}= 0.003. The factor β defined by ACI 318-14 is given as follows:

$$\beta = 0.85 \quad (f_c' \le 30\text{MPa}) \qquad (2)$$

$$\beta = 0.85 - 0.05\frac{(f_c^{'} - 30)}{7} \geq 0.65 \quad (f_c^{'} \geq 30\text{MPa}) \qquad (3)$$

The ERSB in the China Code (GB 50010-2010) is explained using α and β parameters. Factor α and β should be taken as 1.0 and 0.80 for concrete strength grade up to and including C50 (cube concrete strength f_{cu}'=50 MPa), respectively. For concrete strength grade of C80 (cube concrete strength f_{cu}'=80 MPa), factor α and β can be taken as 0.94 and 0.74, respectively. While for concrete strength grade between C50 and C80, parameters α and β should be determined by linear interpolation method. The concrete ultimate compression strain is taken as ε_{cu}= 0.0033.

Canada Code of CSA A23.3-04 defines the ERSB using factors α and β as taken as follows:

$$\alpha = 0.85 - 0.0015 f_c^{'} \geq 0.67 \qquad (4)$$

$$\beta = 0.97 - 0.0025 f_c^{'} \geq 0.67 \qquad (5)$$

The specified concrete compressive strength ranges from 20 MPa to 80 MPa. The ultimate compression strain is taken as ε_{cu}= 0.0035.

As shown in Table 4, the ratios of P_{max} to P_{ACI} was 1.03 on average, ranging from 0.91 to 1.15, the ratios of P_{max} to P_{GB} was 0.91 on average, ranging from 0.83 to 0.99, the ratio of P_{max} to P_{CSA} was 1.04 on average, ranging from 0.93 to 1.15. Theoretical loads of columns obtained according to Code of GB 50010-2010 were larger than experimental maximum loads. Theoretical loads calculated using Codes of ACI 318-14 and CSA A23.3-04 were close to experimental results, and the standard deviations of mean ratios were 0.074 and 0.071, respectively. The average ratio of experimental maximum load to theoretical load obtained using codes decreased with the increase of nominal eccentricity. In the theoretical calculations of columns with high-strength steel, using the ERSB parameters given in Codes of ACI 318-14 and CSA A23.3-04 were more suitable than Code of GB50010-2010.

To evaluate the effects of test design parameters on the post-peak deformability and ductility of columns, the deformability factor λ [27] and ductility index μ [28] are used and presented in Table 4. The deformability factor λ is defined as the ratio of mid-height lateral displacement at ultimate load to mid-height lateral displacement at peak load. The ultimate load was determined by the load corresponding to 85% of maximum load on the descending branch [29]. The ductility index μ is defined as the ratio of ultimate lateral displacement to notional yield displacement. The yield displacement was given as the displacement at yield point of load-displacement curves, which can be determined by method proposed by Park et al. (as show in Fig.7).

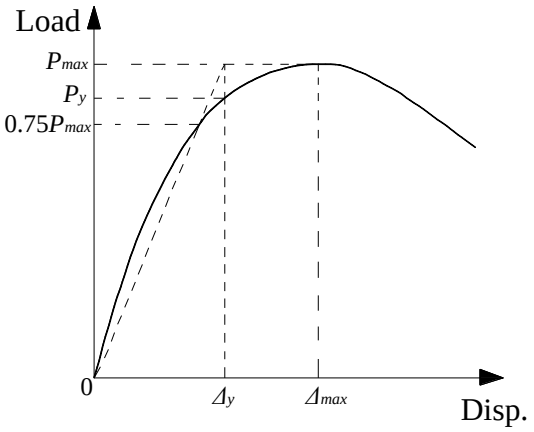

Fig.7 Yield point determined by *Park et al.* method

Table 4 Summary of test results

Column	Axial loads				Mid-height lateral displacements			Deformability	Ductility
	P_{max} (kN)	P_{max}/P_{ACI}	P_{max}/P_{GB}	P_{max}/P_{CSA}	Δ_y (mm)	Δ_{max} (mm)	$\Delta_{0.85P}$ (mm)	λ	μ

EC1	3125	1.08	0.95	1.12	2.89	8.30	12.05	1.5	4.2
EC2	2927	1.01	0.88	1.04	3.60	13.10	26.45	2.0	7.2
EC3	2709	0.97	0.85	1.00	3.95	10.25	19.85	1.9	5.0
EC4	3311	1.14	0.98	1.14	4.38	9.30	30.45	3.3	7.0
EC5	3434	1.15	0.99	1.15	3.87	8.55	21.90	2.6	5.7
EC6	1467	0.98	0.89	1.00	5.45	8.60	22.80	2.7	4.2
EC7	1437	0.98	0.89	1.00	5.74	8.45	19.60	2.3	3.4
EC8	1373	0.91	0.83	0.93	5.68	8.55	17.30	2.0	3.0
EC9	1599	1.05	0.91	1.01	6.44	13.95	44.20	3.2	6.9
EC10	1549	1.01	0.88	0.97	6.25	8.30	27.35	3.3	4.4

4 Discussion of Test Results

4.1 Effect of transverse reinforcement amount

According to the load-displacement curves of columns illustrated in Fig.5 and test results shown in Table 4, four pairs of columns (EC2 and EC3, EC4 and EC5, EC7and EC8, EC9 and EC10) containing high-strength transverse reinforcement were presented, with each pair having same transverse reinforcement configurations but different amounts. Column EC2 exhibited 8%, 5% and 44% increases in maximum load P_{max}, deformability λ and ductility μ, respectively, compared with Column EC3. Similarity, Column EC4 appeared a 4% decrease in maximum load P_{max}, but 27% and 23% gains in deformability λ and ductility μ, respectively, compared with Column EC5. For columns subjected to nominal eccentricity 180 mm, Column EC7 increased by 5%, 15% and 13% in maximum load P_{max}, deformability λ and ductility μ, respectively, compared with Column EC8. Column EC9 presented a 3% and 57% increase in maximum load P_{max} and ductility μ, respectively, compared with Column EC10. These results demonstrate the beneficial effect of transverse reinforcement amount on the behavior of columns under eccentric loading on the basis of deformability and ductility and also show that the confinement effect of transverse reinforcement is more effective in columns loaded to small eccentricity (e=80 mm) than columns subjected to large eccentricity (e=180 mm). This is due to the larger compression zone depth of critical section for columns loaded to small eccentricity.

4.2 Effect of transverse reinforcement yield strength

The effects of transverse reinforcement yield strength on eccentric compressive behavior of columns were shown in Fig.5 and Table 4. Column EC2 with 1.91% of high-strength transverse reinforcement exhibited 33% and 71% increases in deformability λ and ductility μ, respectively, compared with Column EC1with 1.91% of ordinary transverse reinforcement. These results indicate that increasing transverse reinforcement yield strength has beneficial effects on the post-peak deformability and ductility of columns subjected to small eccentricity. However, Column EC7 with 1.91% of high-strength transverse reinforcement showed 15% and 19% decreases in deformability λ and ductility μ, respectively, compared with Column EC6 with 1.91% ordinary transverse reinforcement. This is because the transverse reinforcement cannot yield despite of the use of high-strength transverse reinforcement in columns (refer to measured strains in Table 3). In addition, Columns EC3 and EC8 were detailed with high-strength transverse reinforcement but have smaller transverse reinforcement amount (ρ_{sh}=1.27%) than Columns EC1 and EC6 (ρ_{sh}=1.91%), respectively. Columns EC3 and EC8 exhibited 14% and 7% decreases in maximum load P_{max} compared with Columns EC1 and EC6, respectively. This is attributed to the smaller mechanical ratio ($\rho_{sh}f_{yh}/f_c$') proposed by Canbay et al. [30]. Column EC3 showed 26% and 19% increases in deformability λ and ductility μ, respectively, compared with EC1, although it contained a lower transverse reinforcement amount. However, Column EC8 exhibited 26% and 29% decreases in deformability λ and ductility μ, respectively, compared with Column EC6. These results show that the same level of deformability and ductility only can be achieved with lower amount of transverse reinforcement when high-strength transverse

reinforcements are used in columns subjected to small eccentricity. That is, the beneficial effects of using high-strength transverse reinforcement for the solution of steel congestion of columns can be achieved for columns subjected to small eccentricity. Therefore, the confinement effect of high-strength transverse reinforcement was not effective in columns subjected to large eccentricity.

4.3 Effect of longitudinal reinforcement yield strength

The influences of longitudinal reinforcement yield strength on the behavior of columns were illustrated in Fig.5 and Table 4. Columns EC4, EC5, EC9 and EC10 with high-strength longitudinal reinforcements exhibited 13%, 27%, 11% and 13% increases in maximum load P_{max} compared with Columns EC2, EC3, EC7 and EC8, respectively. These results demonstrate that the high-strength longitudinal reinforcements can increase the bearing capacity of columns. That is, the beneficial effects of using high-strength longitudinal reinforcement for the solution of steel congestion of columns with large amount of reinforcement can be achieved. Columns EC4 and EC5 exhibited similar ductility μ (actually 3% decrease and 9% increase, respectively) compared with Columns EC2 and EC3, respectively. While Columns EC9 and EC10 increased by 103% and 47% in ductility μ compared with Columns EC7 and EC8, respectively. These results indicate that the benefits of using high-strength longitudinal reinforcements for improving ductility can be achieved in columns subjected to large eccentricity. In addition, Columns EC4, EC5, EC9 and EC10 showed 65%, 37%, 39% and 65% increases in deformability λ compared with Columns EC2, EC3, EC7 and EC8, respectively, which indicate that the high-strength longitudinal reinforcement can obviously improve post-peak deformability of columns.

5 Axial Load-Bending Moment Interaction Diagrams

5.1 Bending moment *M*

The behavior of columns with varying design parameters cannot be fully covered experimentally. Hence, numerical models were established using Software Opensees to extensively investigate the effect of concrete strength f_c', eccentricity e and slenderness ratio λ on bending moment of columns with high-strength steel, including concrete strength f_c'=20MPa, 40MPa and 50MPa under different eccentricity e=80mm, 160mm, 240mm, eccentricity e=40mm, 80mm, 120mm, 160mm, 200mm, 240mm, 280mm and 320mm under concrete strength f_c'=30 MPa, slenderness ratio λ=6, 9, 12 and 15 under different eccentricity e=80mm, 240mm. The FE model is based on Nolinear Beam-Column Elements with fiber sections. Herein, the fiber section includes 52 fibers for the unconfined cover, 144 fibers for the confined core, and one fiber for each longitudinal reinforcing bar. Concrete 02 and Reinforcing Steel materials models in Opensees were used to simulate the concrete and steel constitutive of columns, respectively. Besides, the test results in research literature [31] were also collected for comparison. The bending moment capacities of columns were calculated using the ERSB parameters stated in Codes of ACI 318-14, GB 50010-2010 and CSA A23.3-04. The experimental, simulated and calculated bending moment capacities were summarized in Table5.

Due to the nature of eccentric loading, the axial load produced large bending moment at the mid-height of column. The bending moment capacity M of columns reported in Table 5 consist of the primary moment calculated based on nominal eccentricity and the secondary moment caused by lateral mid-height displacement at maximum load (P-Δ effect). The actual e/h for each series of columns was approximately equal and hence any change in bending moment capacity was due to the test variables. As shown in Table 5, the bending moment capacity caused by test variables decreased as increasing e/h. The average of ratios of experimental and simulation bending moment capacity (M) to bending moment capacity (M_{ACI}) computed using the Code of ACI 318-14, M/M_{ACI} was 1.10, to the bending moment capacity (M_{GB}) according to Code of GB 50010-2010, M/M_{GB} was 0.98, to the bending moment capacity (M_{CSA}) calculated according to Code of CSA A23.3-04, M/M_{CSA} was 1.07. The bending moment capacity calculated according to Codes of ACI 318-14 and CSA A23.3 were less than experimental and simulation results, which indicates that the calculated results are conservative. While the bending moment capacities calculated by Code of GB 50010-2010 were bigger than the experimental and

simulation results, which shows that the Code of GB 50010-2010 overestimates the bending moment capacity.

Table 5 Experimental and theoretical bending moment capacity of columns

Source	Column		e (mm)	M(kN·m)	M_{GB}(kN·m)	M_{ACI}(kN·m)	M_{CSA}(kN·m)	M/M_{GB}	M/M_{ACI}	M/M_{CSA}
Test results	EC4		78.5	290.7	274.3	241.1	241.9	1.06	1.21	1.20
	EC5		75	287.0	271.3	237.0	237.1	1.06	1.21	1.21
	EC9		179	308.5	306	277.1	291.3	1.01	1.11	1.06
	EC10		178.5	289.4	306	277.1	291.3	0.95	1.04	0.99
Simulation results	f_c' (MPa)	20	80	242.2	212.6	177.5	183.0	1.14	1.36	1.32
		40	160	316.3	322.6	307.2	317.1	0.98	1.03	1.00
		50	240	351.3	363.9	389.4	400.5	0.97	0.90	0.88
		20	80	270.2	240.7	212.3	224.6	1.12	1.27	1.20
		40	160	337.5	347.1	325.7	361.1	0.97	1.04	0.93
		50	240	373.1	381.8	393.6	426.3	0.98	0.95	0.88
		20	80	270.0	252.2	224.8	240.4	1.07	1.20	1.12
		40	160	318.2	327.6	318.3	333.8	0.97	1.00	0.95
		50	240	343.5	349.2	360.1	375.0	0.98	0.95	0.92
	e (mm)		40	188.1	199.8	172.9	168.6	0.94	1.09	1.12
			80	284.9	275	242.1	243.0	1.04	1.18	1.17
			120	304.6	293.6	264.9	272.6	1.04	1.15	1.12
			160	310.6	302.9	274.2	286.8	1.03	1.13	1.08
			200	304.5	308.3	279.6	292.7	0.99	1.09	1.04
			240	293.8	299.5	281.0	285.1	0.98	1.05	1.03
			280	285.1	292.5	272.9	278.4	0.97	1.04	1.02
			320	277.6	287	266.5	273.1	0.97	1.04	1.02
	λ	6	80	286.7	276.8	248.8	250.8	1.04	1.15	1.14
		9	80	282.4	280.9	260.6	265.8	1.01	1.08	1.06
		12	80	292.3	286.7	270.9	281.1	1.02	1.08	1.04
		15	80	287.6	293	277.5	291.9	0.98	1.04	0.99
		6	240	292.0	298.1	279.0	283.5	0.98	1.05	1.03
		9	240	287.7	294.6	274.7	280.1	0.98	1.05	1.03
		12	240	281.1	288.8	269.2	275.6	0.97	1.04	1.02
		15	240	275.3	281.6	264.2	271.4	0.98	1.04	1.01
Literature [31]	PZ1		210	152.7	150.5	150.0	145.1	1.01	1.02	1.05
	PZ2		230	204.9	203.7	192.0	191.6	1.01	1.07	1.07
	PZ3		150	256.2	232.7	209.0	221.5	1.10	1.23	1.16
	PZ4		210	204.1	210.1	189.5	197.3	0.97	1.08	1.03
	PZ5		210	270.3	240.5	217.9	226.8	1.12	1.24	1.19
	PZ6		120	180.5	180.9	165.2	167.8	1.00	1.09	1.08
	PZ7		220	251.6	234.5	215.6	221.2	1.07	1.17	1.14
	PZ8		170	197.5	174.1	172.2	167.9	1.13	1.15	1.18
	PZ9		120	226.6	213.3	193.7	200.0	1.06	1.17	1.13
	PZ3-2		150	264.4	267.9	247.0	259.7	0.99	1.07	1.02
	PZ5-2		210	277.3	237.6	220.2	223.2	1.17	1.26	1.24
Average								0.98	1.10	1.07

Peer-reviewed version available at Materials 2019, 12, 2139; doi:10.3390/ma12132139

5.2 *P-M* curve diagram

According to the detailed parameters of columns given in the test, the axial load *P* and bending moment *M* of columns can be calculated in terms of relevant formulas of Codes (GB50010-2010, ACI318-14, CSA A23.3-04). For different eccentricity, it can be concluded that the axial load-bending moment (*P-M*) curves were shown in Fig.8. The *P-M* interaction curves calculated using Code of GB 50010-2010 give an upper bound, *P-M* interaction curves obtained using Code of ACI 318-14 almost coincide with CSA A23.3-04 curves. The results remain on the unsafe side of the *P-M* curve obtained using Code of GB 50010-2010, whereas the experimental and simulation points are close to the ACI 318-14 and CSA A23.3-04 curves. The Codes of ACI 318-14 and CSA A23.3-04 give the safe predictions. The Code of GB 50010-2010 overestimates the capacity for columns with high-strength steel. In general, capacities calculated using the Codes of ACI 318-14 and CSA A23.3-04 agree well with test results.

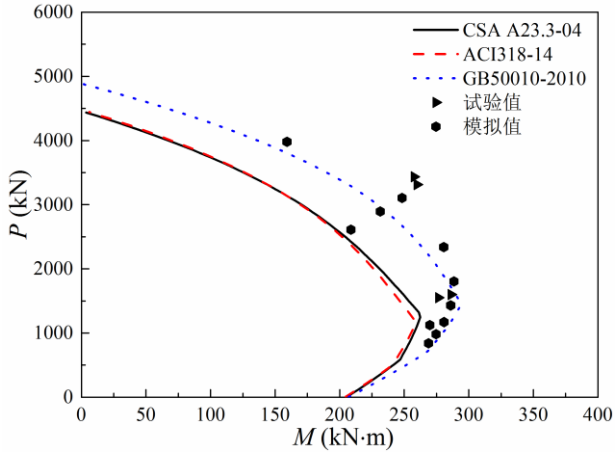

Fig.8 *P-M* curve diagrams of columns with high-strength steel

6 Conclusions

This research aims to study the eccentric compressive behavior of RC columns with new developed high-strength steel. Transverse reinforcement amount and yield strength, eccentricity, and longitudinal bar yield strength are the test variables. In total, ten concrete columns were tested under eccentric loading. According to the experimental and analytical results, some conclusions can be obtained:

1. For small-eccentrically loaded concrete columns reinforced with high-strength steel, the failure localized into the middle part with concrete crushing at the compression-side, which appear compression failure. For large-eccentrically loaded concrete columns with high-strength steel, the tensile cracks extend to the entire cross-section of columns with several major cracks at the tensile zones and concrete crushed at the compression-side, which is typical tensile failure mode.

2. The increasing amount of transverse reinforcement improves the deformability and ductility for columns with high-strength steel. And the confinement effect of transverse reinforcement is more effective in columns subjected to small eccentricity than columns subjected to large eccentricity.

3. The same level of deformability and ductility can be achieved with lower amount of transverse reinforcement when high-strength transverse reinforcements are used in columns subjected to small eccentricity. However, increasing transverse reinforcement yield strength fail to improve post-peak deformability and ductility of column subjected to large eccentricity due to the inadequate confinement of high-strength transverse reinforcement.

4. The high-strength longitudinal reinforcements can improve the bearing capacity and post-peak deformability of columns under eccentric loading, but the benefits of using high-strength longitudinal reinforcements for improving ductility only can be achieved in columns subjected to large eccentricity.

5. In general, the equivalent rectangular stress block (ERSB) parameters stated in Code of GB 50010-2010 overestimates the bearing capacity of columns with high-strength steel, whereas bearing capacities computed using Codes of ACI 318-14 and CSA A23.3-04 agree better with test results.

Acknowledgments

The authors would like to express their gratitude to Natural Science Foundation of Jiangsu Province (BK20171361) for financial support and to Key Laboratory of Concrete and Prestressed Concrete Structures of Ministry of Education, Southeast University, P.R. China for technical support.

References

[1] Tavallali H, Lepage A, Rautenberg JM, Pujol S. Concrete beams reinforced with high-strength steel subjected to displacement reversals. ACI Structural Journal 2014; 111(5): 1037-1047.

[2] Ibarra L, Bishaw B. High-strength fiber-reinforced concrete beam-columns with high-strength steel. ACI Structural Journal 2016; 113(1): 147-156.

[3] Wibowo LSB, Cheng MY, Huang FC, Tai TY. Effectiveness of high-strength hoops in high-strength flexural members. ACI Structural Journal 2017; 114(4): 887-897.

[4] Hwang HJ, Park HG, Choi WS, Chung L, Kim JK. Cyclic loading test for beam-column connections with 600 MPa (87 ksi) beam flexural reinforcing bars. ACI Structural Journal 2014; 111(4): 913-924.

[5] Alaee P, Li B. High-strength concrete interior beam-column joints with high-yield-strength steel reinforcements. Journal of Structural Engineering 2017; 143(7): 1-12.

[6] Lee HJ, Chang CJ. High-strength reinforcement in exterior beam-column joints under cyclic loading. ACI Structural Journal 2017; 114(5): 1325-1338.

[7] Park HG, Baek JW, Lee JH, Shin HM. Cyclic loading tests for shear strength of low-rise reinforced concrete walls with grade 550 MPa bars. ACI Structural Journal 2015; 112(3): 299-310.

[8] Cheng MY, Hung SC, Lequesne RD, Lepage A. Earthquake-resistant squat walls reinforced with high-strength steel. ACI Structural Journal 2016; 113(5): 1065-1076.

[9] Rautenberg JM, Pujol S, Tavallali H, Lepage A. Reconsidering the use of high-strength reinforcement in concrete columns. Engineering Structure 2012; 37: 135-142.

[10] Rautenberg JM, Pujol S, Tavallali H, Lepage A. Drift capacity of concrete columns reinforced with high-strength steel. ACI Structural Journal 2013; 110(2): 307-317.

[11] Ou YC, Kurniawan DP. Shear behavior of reinforced concrete columns with high-strength steel and concrete. ACI Structural Journal 2015; 112(1): 35-45.

[12] Ou YC, Kurniawan DP. Effect of axial compression on shear behavior of high-strength reinforced concrete columns. ACI Structural Journal 2015; 112(2): 209-219.

[13] Sokoli D, Ghannoum WM. High-strength reinforcement in columns under high shear stresses. ACI Structural Journal 2016; 113(3): 605-614.

[14] Trejo D, Link TB, Barbosa AR. Effect of reinforcement grade and ratio on seismic performance of reinforced concrete columns. ACI Structural Journal 2016; 113(5): 907-916.

[15] Li B, Park R, Tanaka H. Stress-strain behavior of high-strength concrete confined by ultra-high- and normal-strength transverse reinforcements. ACI Structural Journal 2001; 98(3): 395-406.

[16] Han BS, Shin SW, Bahn BY. A model of confined concrete in high-strength reinforced concrete tied columns. Magazine of Concrete Research 2003; 55(3): 203-214.

[17] Legeron F, Paultre P. Uniaxial confinement model for normal-and high-strength concrete columns. Journal of Structural Engineering 2003; 129: 241-252.

[18] Paultre P, Legeron F, Mongeau D. Influence of concrete strength and transverse reinforcement yield strength on behavior of high-strength concrete columns. ACI Structural Journal 2001; 98(4): 490-501.

[19] Xiao X, Guan FL, Yan S. Use of ultra-high-strength bars for seismic performance of rectangular high-strength concrete frame columns. Magazine of Concrete Research 2008; 60(4): 253-259.

[20] Lepage A, Tavallali H, Pujol S, Rautenberg JM. High-performance steel bars and fibers as concrete

reinforcement for seismic-resistant frames. Advances in Civil Engineering; 2012: 1-13.

[21] Link TB. Seismic performance of reinforcement concrete bridge columns constructed with grade 80 reinforcement. Master's thesis, Oregon State University; 2014.

[22] American Concrete Institute (ACI). Building code requirements for structural concrete and commentary. ACI 318-14, Detroit; 2014.

[23] Lloyd NA, Rangan BV. Studies on high-strength concrete columns under eccentric compression. ACI Structural Journal 1996; 93(6): 631-638.

[24] Claeson C, Gylltoft K. Slender high-strength concrete columns subjected to eccentric loading. Journal of Structural Engineering 1998; 124(3): 233-240.

[25] China National Standard. Code for design of concrete structures. GB 50010-2010, Beijing; 2010.

[26] Canadian Standards Association (CSA). Design of concrete structures. CSA A23.3-04, Ontario; 2004.

[27] Wang L, Su RKL. Theoretical and experimental study of plate-strengthened concrete columns under eccentric compression loading. Journal of Structural Engineering 2013; 139(3): 350-359.

[28] Hadi MNS, Widiarsa IBR. Axial and flexural performance of square RC columns wrapped with CFRP under eccentric loading. Journal of Composite Construction 2012; 16(6): 640-649.

[29] Gangarao HVS, Taly N, Vijay PV. Reinforced concrete design with FRP composites. CRC, London; 2007.

[30] Canbay E, Ozcebe G, Ersoy U. High-strength concrete columns under eccentric load. Journal of Structural Engineering 2006; 132(7): 1052-1060.

[31] Luo SH. Experimental study on behavior of eccentrically loaded RC members with 600MPa steel bars. Master's thesis, Southeast University; 2013.